Application of a multi-winding magnetic component characterization method to optimize cross-regulation performances in DCM flyback converters

Denis MOTTE-MICHELLON[1,2], Brahim RAMDANE[2], Yves LEMBEYE[2],
Bruno COGITORE[1]
EXXELIA/G2ELAB
[1]Exxelia R&D center: 137 rue Mayoussard, ZA Centr'Alp, 38 430 Moirans, France
[2]Univ. Grenoble Alpes, CNRS, Grenoble-INP*, G2Elab, 38 000, Grenoble, France
Tel.: +33 / (0) – 476.35.05.92
E-Mail: denis.motte-michellon@g2elab.grenoble-inp.fr
URL: https://exxelia.com

Keywords

Multiple secondary windings, Device characterization, Flyback converter, Transformer, DC voltage control.

Abstract

In this paper, output voltage deviations issues in multi-output DCM cross-regulated flybacks are studied, with a particular focus on the transformer. Using the extended Cantilever model, a general explanation of the influence of the transformer on voltage deviations is developed. Then, an application of an analytical model based on a formulation of the magnetic vector potential allowing to characterize the transformer around 1,000 faster than its finite-element method (FEM) equivalent is presented. This characterization method, fast and accurate, offers the possibility to create a design aid tool for the transformer manufacturer, allowing to define the winding layout with the best cross-regulation performances for a transformer taking place in a given converter.

Introduction

Multi-output Discontinuous Conduction Mode (DCM) flybacks have several advantages when it comes to powering several loads with a total power not exceeding ~100W: its low number of components makes it cheap and reliable, and the embedded transformer offers voltage level adaptation thanks to the number of turns, as well as galvanic insulation. Thanks to all these advantages, multi-output DCM flybacks are appreciated by converter manufacturers for low-power space-bound applications.
However these advantages do not come without drawbacks: The simplest and most widely spread method to regulate output voltages in this type of converters is cross-regulation. It means that only one output voltage is closed-loop regulated with action on the duty cycle, while the other output voltages are let free. The idea behind this method is that the regulated output voltage has approximately the same behavior (i.e. the same transfer function V/α, α being the duty cycle) than all the other outputs. Thus, regulating the voltage of this single output should be sufficient to regulate the voltage of all the others, at least approximately.
This hypothesis is sometimes wrong, and cross-regulated outputs (i.e. outputs that are not directly regulated) experience important steady-state voltage deviations, with known examples of voltage excursions up to almost twice the nominal values. The current solution to this problem is to implement linear regulators on outputs for which voltage deviations are not acceptable, such as sensitive high-end sensors. Nevertheless, this solution is especially unsatisfying for space industry because it leads to adding extra subsystems to the converter, consequently increasing cost, complexity, weight and possible failure sources.

*Institute of Engineering Grenoble-Alpes

Transformers were known to be part of the causes of cross-regulation failures. Thus, our work aimed at understanding how the magnetic component influences output voltages deviations in order to propose design recommendations, and ultimately a design optimization tool for the transformer designer.
In this paper, an analysis of the influence of the transformer on cross-regulation is first presented. Then an analytical modeling method for characterizing the transformer is developed for the purpose of creating a reliable and fast design optimization tool for the transformer designer.

I – Global model of cross-regulation

I.1 – Context, method and objectives

In this study, the objective was to find out how to design multi-output flyback DCM in order to reduce the magnitude of voltage deviations due to cross-regulation imperfections. Focus was put on the magnetic component, since it is known to have a significant influence on cross-regulation performances, especially through the set of all its magnetic couplings – which can also be interpreted as leakage inductances. From a behavioral model of the transformer, an analysis of the influence of the magnetic phenomena was conducted through analytical calculations and a consistent correlation was found.

In order to confirm the conclusions that were drawn, characterizations of the behavioral model of several versions of one transformer were conducted on a finite elements method (FEM) software. All the versions of the transformer were featuring the same winding set. Number of turns and copper section are identical for each winding from one version to another. Only their positions in the frame were different. This method allowed the modification of only the magnetic couplings between the windings while keeping the other parameters unchanged between the several versions. Then, simulations of the operation of the converter with the models of the several versions were conducted in a circuit simulation software (PSIM), which allowed to compute output voltages on several operating points, highlighting the influence of the transformer on output voltage deviations. This approach allowed to find a link between the winding layout and the transformer influence on the cross-regulation performances. Thus, transformer design recommendations were formulated in accordance with the analysis of the phenomena.
However, the FEM characterization method, albeit precise, is much too slow to explore all the possible layouts or to run an optimization method in the general case. Indeed, the number of possible versions of the transformer is equal to N!, with N being the number of elements whose positions can be permutated. Let us take the example of a transformer featuring 10 different layers of windings. The number of versions that can be obtained for this transformer is 10! = 3 628 800, which is way too much to be comprehensively explored in a reasonable time. Thus, another goal was to find an analytical model of the magnetic energy in the transformer window that could be used to characterize the equivalent circuit model, in order to reach faster computation time than the FEM formulation. Two analytical magnetic energy models were compared to the FEM formulation, taken as the reference. One of these two models revealed to be accurate enough and around one thousand times faster than the FEM model, unlocking the possibility to develop a winding layout optimization tool to achieve transformer design with better cross-regulation performances.

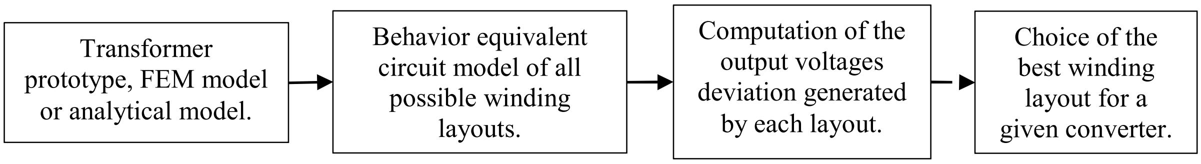

Fig. 1: Method used to analyze cross-regulation performances of different winding layout on a transformer

I.2 – Model of the transformer

In order to represent the behavior of the transformer (i.e. the relationships between the voltages across the windings and the current flowing through them), we chose to use a magnetic quasi-static model excluding energy losses in the transformer and capacitive effects.

For stray capacitances, this simplification was made under the assumption that magnetic phenomena have a much greater impact on transformer behavior than capacitive effects. Electric energy is of course stored along with magnetic energy, since electric field develops between windings. However flybacks typically operate under 500kHz, which is under the typical no-load resonant frequencies of windings (around some MHz), meaning the modules of the impedances of the inductances are lower than the modules of the impedances of the stray capacitances. On the other hand, simulations showed that the winding resistances had little influence on the cross-regulation phenomenon. Thus, a model including only inductances seemed adapted to model properly the transformer behavior.

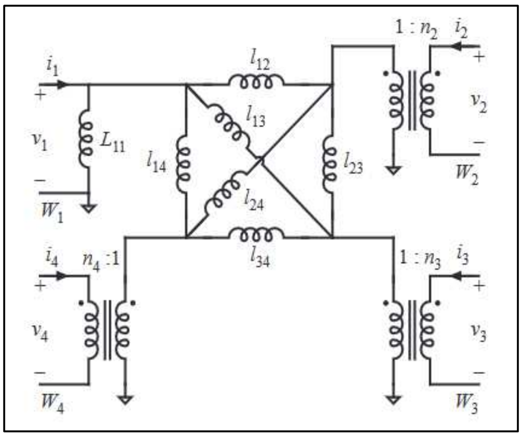

Fig. 2: Extended Cantilever model, four-winding example

The extended Cantilever model [1] was chosen. This model is equivalent to the inductance matrix, meaning it contains the same information about the transformer behavior – i.e. it has the same number of independent parameters. Fig. 2 shows an example of the structure of the model for a four-winding magnetic component.
The particularity of this model is that it models all the couplings between all windings thanks to leakage inductances placed between every couple of windings. One of its advantages is that it allows an easy comparison of the values of the couplings between windings, since all the leakage inductance are placed on the side of a single winding. What is more, the formulation of the couplings by leakage inductances allows to write easily formulas describing energy flows between windings, leading to the simplified analytical model presented in §II.1

II – Simplified model of the voltage deviations on the lowest power output

II.1 – Observations and hypotheses

In DCM cross-regulated multi-output flybacks, voltage deviations are most often observed on voltage rises on low-power secondaries. Thus, focus was put on modeling this particular phenomenon with an analytical formula that could give a physical interpretation of the phenomenon.
A four-winding flyback transformer was characterized to obtain the values of the parameters of its Cantilever model. This allowed us to run simulations of a simple three-output flyback converter.

In order to work with expressions of reasonable complexity, a number of classical simplifying hypotheses were made: output voltages are constant with no voltage ripple – steady state is reached and the output capacitors have very high values compared to the power consumption of the loads they feed. Converter components are ideal, and there is no energy dissipation in any of the converter's component neither in the transformer. In addition, there is no snubber circuit on the primary of the converter, hence the current is transferred instantaneously from the primary to the secondaries when the MOS opens at αT – with α being the duty cycle and T the duration of the period of the converter. A two-output example is displayed on Fig. 3:

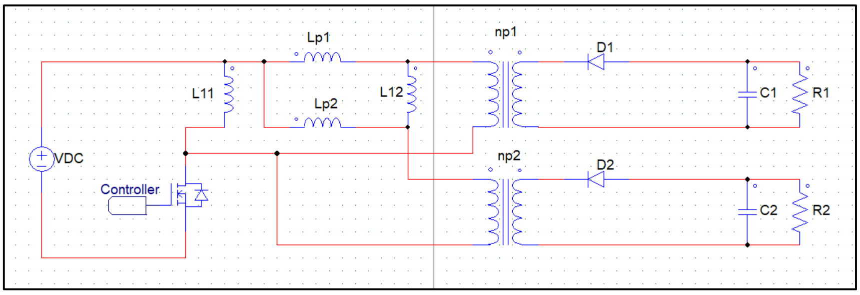

Fig. 3: Structure of a simplified two-output flyback

From the simulations, we obtain the secondary current waveforms shown on fig. 4. These broken lines current waveforms are also shown in [3] and [4]. In [3] the author uses the same hypotheses – except for the primary snubber – to obtain analytical formulas of the voltages outputs, but they are extremely cumbersome for a flyback with only two outputs, and we could not deduce a physical explanation from them.

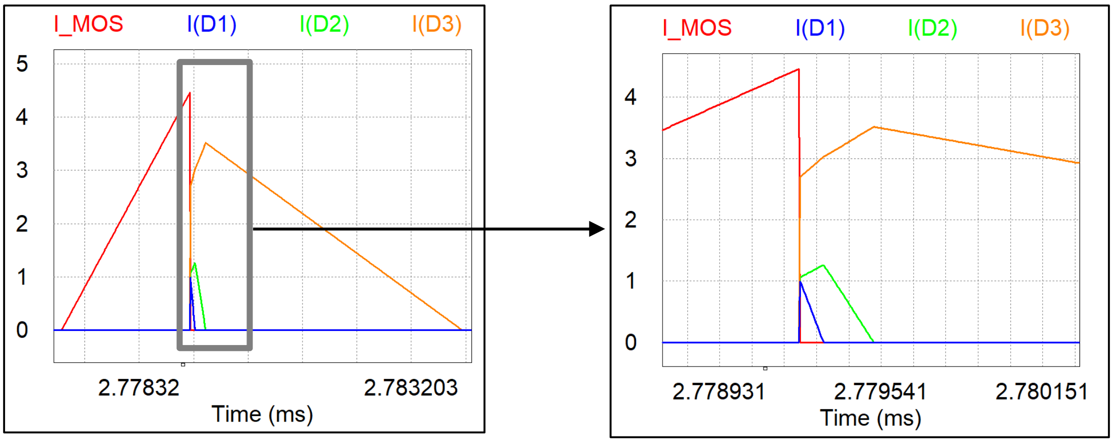

Fig. 4: (a) Current waveforms in the primary MOS and in the diodes of secondary windings obtained in a PSIM simulation. (b) Zoom on the beginning of the demagnetization phase.

An important thing to notice is that with these hypotheses, the current in a secondary k at αT^+ – just after the MOS switches to its blocked state – does not depend of the power of the load of the output k in any way. Instead, it depends on i_p, the current in the primary at αT^- and on the leakage inductance between the primary and the secondary k compared to the other leakage inductances. It is expressed in (1):

$$i_k(\alpha T^+) = i_p(\alpha T^-) \cdot \frac{\frac{1}{L_{pk}}}{\sum_{j=1}^{N} \frac{1}{L_{pj}}} \tag{1}$$

II.2 – Equivalent circuit of the magnetic phenomena

From the PSIM simulations and the waveforms of the fig. 4 (b), one can notice that the current of the lower-power secondary #1 is the first to fall to zero. Since the secondary #1 drives current for a very short duration, it has little time to exchange energy with the two other secondaries. We make the hypothesis that there is no direct exchange of energy between this secondary and the others, since the conduction time of the secondary #1 is very short. In the Cantilever model, energy exchanges between secondary windings would be modelled by currents flowing through the leakage inductance connecting the secondary windings. Since they are assumed negligible, the equivalent circuit describing the situation of the low-power output during its conduction time is presented on Fig. 5:

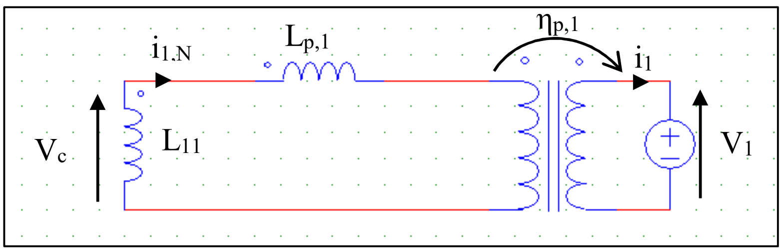

Fig. 5: Circuit describing the situation of the lowest power output during its conduction time.

V_c is the voltage at the terminals of the magnetizing inductance of the transformer. Physically speaking, it expresses the variation of the magnetic flux common to all windings. With the Cantilever model, its expression is found by expressing the equality of the current in the magnetizing inductance L_{11} and the sum of the currents in the leakage inductances:

$$\forall\, t, i_{L11}(t) = \sum_{k=1}^{M} i_{k,N}(t) \tag{2}$$

Then, deriving (2) with respect to time (in (3)) and expressing the derivatives of the currents as a function of the voltages across the inductances (in (4)) yields an expression linking V_c and the voltages of all the outputs:

$$\forall\, t, \frac{d\, i_{L11}(t)}{dt} = \sum_{k,\ i_k(t)\neq 0} \frac{d\, i_{k,N}(t)}{dt} \tag{3}$$

$$\forall\, t, \frac{V_c(t)}{L_{11}} = \sum_{k,\ i_k(t)\neq 0} \frac{\frac{V_k(t)}{\eta_{p,k}} - V_c(t)}{L_{p,k}} \tag{4}$$

It is important to note that only the secondary windings in which the current is non-zero are taken into account in this expression. If the current in a secondary winding falls to zero, the diode of its outputs becomes blocked, thus the current remains zero and its derivative is zero. Consequently the secondary has no more influence on the voltage across the magnetizing inductance. Finally, transforming (4) gives us the expression of V_c as a function of the output voltages, the magnetizing inductance and the leakage inductances between the primary and all the secondary windings:

$$\forall\, t, V_c(t) = \frac{\sum \frac{V_k(t)}{\eta_{p,k} \cdot L_{p,k}}}{L_{11} + \sum L_{p,k}} \tag{5}$$

II.3 – Analytical expression of the output voltage

Now that V_c is expressed, let us proceed to the expression of V_1 as a function of the parameters of the converter. With the assumption we have made, at the time αT^+ the current i_1 has a non-zero value, and so does the current $i_{1,N}$. Since the current $i_{1,N}$ is flowing through the inductance $L_{p,1}$, its derivative with respect to time can be expressed in (6):

$$\forall\, t, \frac{di_{1,N}(\mathrm{t})}{dt} = \frac{V_c(T) - \frac{V_1(t)}{\eta_{p,1}}}{L_{p,1}} \tag{6}$$

Since V_c and V_1 are constants over the period of the converter that is considered, the current $i_{1,N}$ (and thus the current i_1) decreases at a constant pace ($V_1/\eta_{p,1}$ is greater than V_c) until it falls to zero. Thus, the current i_1 has the shape of a triangle, of base $(\beta_1 - \alpha)T$ and a maximal value at αT, given by (1). $\beta_1 * T$ is the time when the current i_1 falls to zero, so β_1 is the duty cycle of the diode of the output #1, D1. It is given by (7):

$$\beta_1 \cdot T = \alpha \cdot T + \frac{i_1(\alpha \mathrm{T}^+)}{\frac{V_c - V_{1,N}}{L_{p,1}}} \tag{7}$$

Expressing the duty cycle of D1 allows us to express the average value of the current through the secondary winding. Assuming that the load of the output is a resistor of value R_{load1} under the voltage V_1, and that the steady state of the output #1 is reached, the average current in the load and the average of the current in the secondary #1 over a period of the converter are the same. The equality between the average current in the winding and the average current in the load is written in (8). Solving the obtained 2[nd]-order polynomial with V_1 as the unknown yields the result exposed in (9):

$$\frac{1}{T}\cdot\frac{1}{2}\cdot i_1(\alpha T^+)\cdot(\beta_1 T-\alpha T)=\frac{V_1}{R_{Load1}} \tag{8}$$

$$V_1=\frac{\eta_{p1}}{2}\cdot\left(V_c+\sqrt{{V_c}^2+\frac{2\cdot R_{load1}\cdot i_p(\alpha T^-)^2\cdot\frac{1}{L_{p,1}}}{T\cdot\left(\sum_{k=1}^{N}\frac{1}{L_{p,k}}\right)^2}}\right) \tag{9}$$

II.4 – Physical interpretation of the formula

Even though this formula is obtained from strong simplifying hypotheses, we deduce the following physical interpretation: The power distributed to the output #1 by the flyback strongly depends on the magnetic couplings in the transformer – expressed in the previous formulas under the form of leakage inductances. Thus, if the transformer has a set of couplings that makes the output #1 receive more power than it is supposed to consume in nominal conditions, the voltage of the output #1 will experience a steady-state overvoltage. The bigger R_{load1} is, meaning the smaller the power consumed by the load of the output #1 is, the higher the output voltage is likely to rise over its nominal value.
This formula also illustrates the influence of the outputs between them: if the total power supplied by the flyback does increase, meaning the duty cycle of the MOS increases, the value of $i_p(\alpha T^-)$ will also increase. If the power consumption of the load of the output #1 remains the same, its voltage will rise due to the increased power received.
For this particular case the solution is to increase the leakage inductance L_{p1} – meaning that the magnetic coupling between the primary and the secondary 1 is weakened. This effect is due to the fact that increasing the inductance L_{p1} leads to a lower value of $i_1(\alpha T^+)$, meaning that the secondary #1 receives a smaller amount of energy after the MOS opens. Hence, cross-regulation performances can be improved by designing the transformer in order to obtain appropriate magnetic couplings between all windings, so the energy is distributed to outputs according to their respective needs.

III – Extended explanation of the influence of the transformer

III.1 – Energy exchanges between secondary windings

According to the models of the converter and the transformer presented above, works in the converter as an energy dispatcher, and its effects depend on the magnetic couplings between all the windings, since they all can exchange energy. Consequently, the energy dispatch can only be correctly modeled if the transformer model contains as much information as the inductance matrix of the transformer – i.e. the model of a transformer with N windings must feature at least N(N+1)/2 independent parameters.

§II exposes the influence of the couplings between primary and secondary windings, since they control the energy dispatch when the current is transferred from the primary to the secondary windings. Another effect that influences output voltage deviations is the exchange of energy between the secondary windings during the demagnetization phase. Indeed, if two secondary windings both drive current during a time $T_{j,k}$, they may exchange energy. Since the secondary windings stop driving current one after another, $T_{j,k}$ is equal to the duration of the conduction time of the secondary that stops driving current first among j and k, as it is expressed in (11).
In order to simplify the notations, let us use the secondary voltage of the output k referred to the primary $V_{k,prim}$, defined by (10):

$$V_{k,prim}(T) = \frac{V_k(t)}{\eta_{p,k}} \tag{10}$$

With V_k being the voltage of the output k and $\eta_{p,k}$ the turn ratio between the primary and the secondary k. If there is a difference between the voltages of two outputs j and k referred to the primary, the secondary j will give to the secondary k an energy $W_{j,k}$, given by (11):

$$W_{j,k} = \frac{(V_{j,prim} - V_{k,prim})^2 \cdot (\min(\beta_j, \beta_k) \cdot T_c)^2}{L_{jk}} \tag{11}$$

With $L_{jk} = L_{kj}$ being the effective leakage inductance between the winding j and the winding k in the Cantilever model. The energy goes from the output having the highest normalized voltage to the output having the lowest. Thus, this effect tends to bring normalized voltages towards a common value, meaning it reduces voltage deviations. What comes from the formula (11) is also that decreasing the value of the inductance L_{jk} – i.e. improving the magnetic coupling between the windings j and k – increases this effect. As a result, another guideline to reduce voltage deviations is to improve as much as possible the coupling between all the secondary windings. This requirement can be contradictory with the need to make magnetic couplings between primary and a secondary proportional to the power of the output fed by this secondary. Thus, our goal is to create a design aid software to help the transformer designer to identify the winding layout with the best cross-regulation performances for a transformer to be put in a given converter. §IV presents the application of an analytical formulation allowing characterizing the inductance matrix in a much faster way than a FEM software, allowing to explore quickly a great number of winding layouts.

III.2 – Validation of the extended explanation

In order to validate the explanation exposed in the paragraph II.3, the method presented in the paragraph I was applied on a four-winding transformer meant to be implemented in a three-output flyback. The transformer is built with an EQ25 magnetic circuit. The windings are wound on a frame on five concentric layers that occupy its whole volume. The primary and the higher power secondary are both wound on two layers, while the two low power secondaries are wound on the same layer as shown in Fig. 6. This distribution of the windings is such that by swapping layers, 5!/(2!*2!) = 30 different versions can be obtained. The Cantilever models of the 30 versions were characterized through FEM simulations.

Then, PSIM simulations of the operation of the converter with the models of the 30 different versions of the transformer were successively made. The three outputs of the simulated converter have very different nominal power consumption, respectively 0.07W for the output #1, 0.35W for the output #2 and 34W for the output #3. During the tests, the voltage of the output #3 was closed-loop regulated to be kept at 28V, its nominal value. Two operating points were tested, one with the output #3 consuming 30% of its nominal power, and the other with the output #3 consuming its nominal power. The load resistors of the outputs #1 and #2 were kept constant and their steady-state voltages monitored, to be compared to their nominal values, 14V for both.

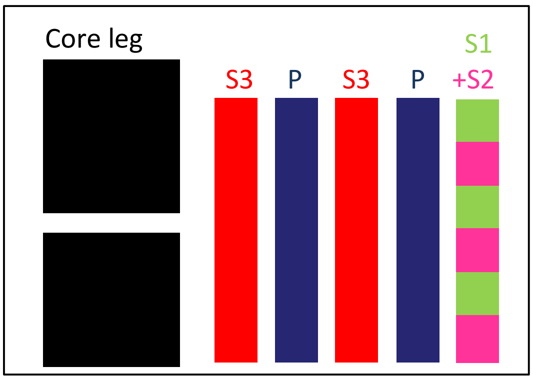

Fig. 6: Example winding layout with average cross-regulation performances.

This approach allowed to characterize the cross-regulation performances of the 30 possible winding layouts for this application. It allowed us to confirm the explanation of the energy dispatch taking place in the multi-output flyback: winding layouts that tended to dispatch power accordingly to each output's need during MOS turn-off and also during demagnetization phase generate the lowest voltage deviations on cross-regulated outputs. Oppositely, those tending to dispatch too much power to cross-regulated outputs resulted in steady-state voltage rises on these outputs. For confidentiality issues, the best and the worst winding layouts for this application cannot be disclosed. Nonetheless, Fig. 7 shows a comparison of the cross-regulation performances of the remarkable winding layouts. These results show that the transformer plays a crucial role in the multi-output flyback, and has a major impact on cross-regulation performance: the best winding layouts generate close to zero voltage deviations (about +1% on

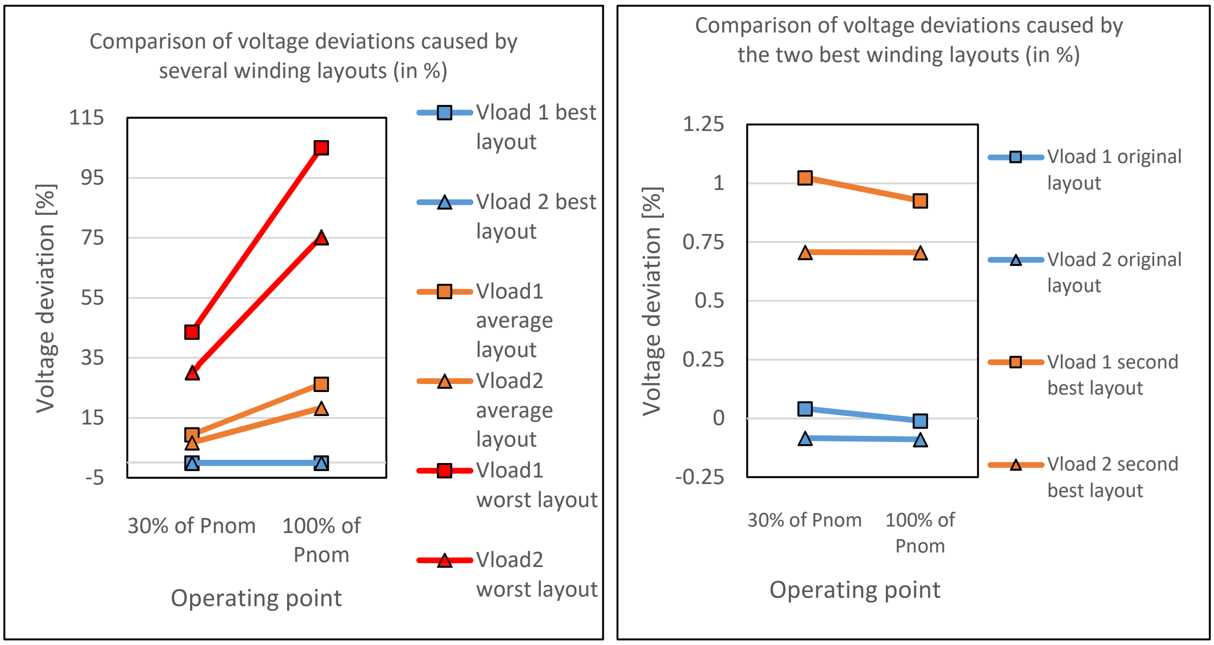

Fig. 7: Comparison of the performances of several winding layouts.

Vload1for the second best layout), while the worst one practically twice the nominal voltage on the least power output (+105% on Vload1 at full power). Consequently, the flyback transformer design should be made with the greatest care, with a great attention given to all the magnetic couplings and not only the number of turns.

IV – An analytical magnetic vector potential model to bypass FEM characterizations

IV.1 – Principle of the model and application

This model is presented in [6]. It is aiming to compute the magnetic energy stored in the transformer during a short-circuit test by computing the interaction between all the conductors thanks to formulas expressing the vector potential generated by the current in the conductors. The values of all short-circuit inductances can be obtained – for tests with a single winding being fed and a single other one being shorted. It is based on the formula of the magnetic energy expressed by magnetic vector potential:

$$W_{mag} = \frac{1}{2} \iiint_{\Omega} \vec{A}\,\vec{J}\; dV \tag{12}$$

With $\vec{A}$ the magnetic vector potential and $\vec{J}$ the current density. The integral is limited to conductors, since the integrated term is worth zero where the current density is zero.

The hypotheses are the following: the problem is considered two-dimensional, the current densities are homogeneous on the section of the conductors, and the sum of ampere-turns in the transformer window equals strictly zero. This situation is equivalent to a short-circuit test with a negligible leakage energy.

Since the problem is considered two-dimensional, the formula (12) is simplified in (13), which expresses the energy per length unit:

$$Wl_{mag} = \frac{1}{2} \iint_{\Omega} \vec{A}\vec{J}\ dS \tag{13}$$

For implementing this computation, a formula expressing the magnetic vector potential field generated by a surface current distribution is provided. Since this model was basically developed to compute the short-circuit inductances in planar transformers, conductors are supposed to be of square shape. It is possible to use the same principle than in [6] to compute magnetic energy with round conductors, it would only take to compute new integrals adapted to this new shape. Nonetheless, we chose to try with formulas developed for square conductors, as it does little difference on the current distribution.

IV.2 – Implementation and results

Based on the formulas provided in [6], a program was created to compute all the short-circuit inductance of one version of the transformer which all possible versions were characterized with a FEM method. Since the goal was to find a characterization method that was faster than a FEM software but still accurate, a comparison of the two methods was realized. The voltage deviations found on PSIM simulations were used as point of comparison, as it is the interesting values for optimizing the cross-regulation performances. The version generating the biggest voltage deviations was used, in order to maximize the differences and obtain a proper comparison between the FEM and the analytical method.

For the analytical method, two different versions were tested: in the first one, all the separate conductors were considered one by one and included in the computations. In the second, winding layers containing the conductors of a single winding – such as P and S3 on Fig. 6 – were modelled as large rectangular conductors. Thus, the first version featured 66 different conductors while the second featured only 10.

For the calculation, all the possible short-circuit tests with one winding fed and one winding shorted are computed in order to obtain the mutual inductances between all the windings. For one short-circuit test, the MATLAB script that was made successively computes the energy generated by the interaction between one conductor and all the others, including itself. What is computed is the interaction between the magnetic vector potential field generated by the conductor k and the current flowing in all the conductors. Every interaction is a piece of the integral expressed in (13) and represents a part of the total magnetic energy stored in the system. Then, when the total magnetic for a short-circuit test is known, the short-circuit inductance seen from the fed winding $L_{shorted}$ is obtained thanks to (14):

$$W_{mag} = \frac{1}{2} L_{shorted} \cdot {I_{fed}}^2 \tag{14}$$

With I_{fed} the current in the fed winding. Then, from the formula (15) given in [2], the formula (16) is obtained and allows to compute the mutual inductance between the winding j and k – with j being the fed winding and k the shorted winding:

$$L_{shorted} = L_j - \frac{{M_{j,k}}^2}{L_k} \tag{15}$$

$$M_{j,k} = \sqrt{L_j \cdot L_k - L_k \cdot L_{shorted}} \tag{16}$$

With L_j and L_k being respectively the self-inductances of the winding j and k. Once the inductance matrix is filled, the extended Cantilever model parameters are computed from formulas given in [1]. Then, a PSIM simulation allows to obtain the output voltages generated by the model of the transformer characterized through the analytical potential vector model. The voltage deviations found in PSIM simulations with the two versions of the transformer model generated by the potential vector model – one with all conductors modelled and the other with complete layers modelled by single conductors – are compared to the voltage deviations generated by the model obtained with FEM characterization, taken as reference on Fig. 8.

These results suggest that even a simplified version of the potential vector model offers a decent precision to characterize the inductance matrix of a transformer. The version where all the conductors are modelled offers an excellent precision, with very little error on the output voltages (maximum 1.13% for the model with all wires and 8.69% for the model with full layers modelled as plates) compared to the results obtained with the model from a FEM characterization with a mesh of about 70k degrees of freedom. What is more, the analytical model proves to be very fast compared to the FEM characterization, about 1,000 faster for the version with all wires modelled, and about 10,000 times faster for the simplified geometry. Thus, this analytical method unlocks the possibility to create a design aid tool exploring a great number of winding version in a reasonable amount of time.

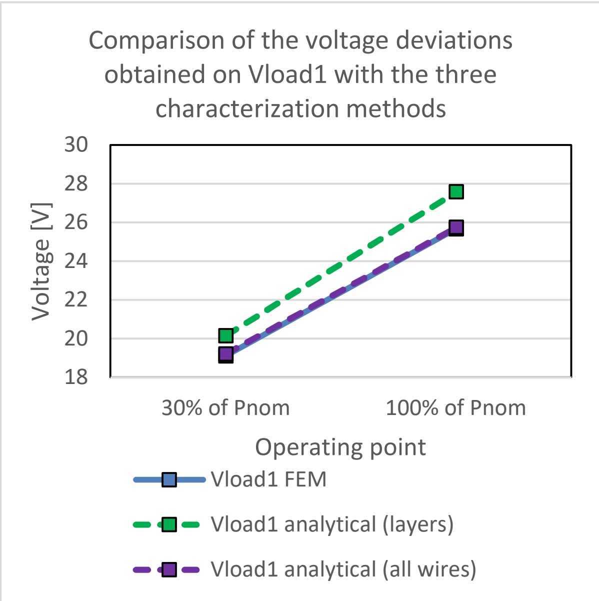

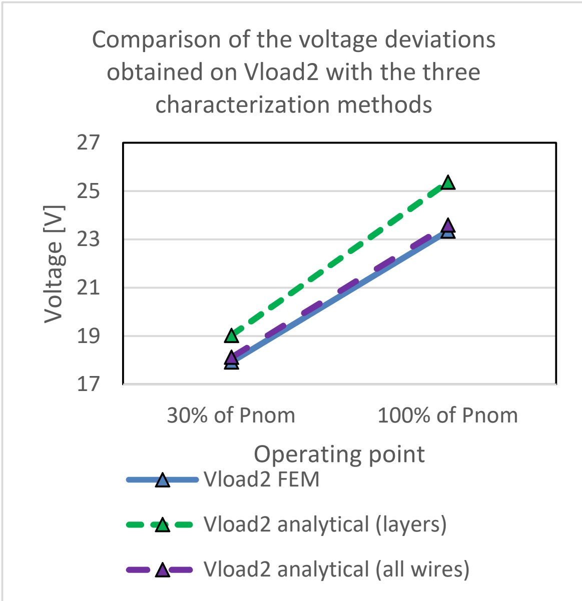

Fig. 8: Comparison of the precision of two versions of the analytical model.

Conclusion

A physical analysis of the influence of the transformer on cross-regulation is presented, as well as guidelines to design transformers that generate less voltage deviations. The analysis is confirmed by the results on a four windings transformer implemented in a three outputs flyback with a great power heterogeneity among the outputs. In order to use it to create an optimization tool, a model allowing to compute short-circuit inductances in transformers thanks to analytical formulas is tested. This model, based on the computation of the magnetic energy thanks to a formulation of the magnetic vector potential in the transformer window has proved to be both fast and accurate. This model allows the creation of a design aid tool for improving cross-regulation performance of transformer in DCM flyback converters in the future.

References

[1] Erickson R. W.: A multiple-winding magnetics model having directly measurable parameters, PESC 98 Record. 29th Annual IEEE Power Electronics Specialists Conference Vol. 2 pp. 1472-1478

[2] Keradec J.P. : Transformateurs HF à enroulements : schémas à constants localisées, Techniques de l'ingénieur, TIP301WEB, D3058 V1

[3] Ji C.: Cross Regulation in Flyback Converters: analytic model and solution, IEEE Transactions on Power Electronics Vol. 16 no 2 pp. 231-239

[4] Hu Y.Q.: Mathematical Modeling of Cross-Regulation Problem in Flyback Converters, 2001 IEEE 32nd Annual Power Electronics Specialists Conference, paper 01CH37230

[5] Chen M.: A Systematic Approach to Modeling Impedances and Current Distribution in Planar Magnetics, IEEE transaction on power electronics Vol. 31 no 1 pp. 560-580

[6] Margueron X.: Complete Analytical Calculation of Static Leakage Parameters: A Step Toward HF Transformer Optimization. Industry Applications, IEEE Transactions on Industry Applications Vol. 46 no 3 pp 1055-1063